

Spectral and entanglement properties of the two-electron Gaussian quantum dot

Arkadiusz Kuroś, Anna Okopińska

Jan Kochanowski University in Kielce, Poland

Critical Stability, Santos 2014



1 Introduction

Outline

- 1 Introduction
- 2 Two-electron anisotropic quantum dot model 3D \rightarrow quasi 1D

Outline

- 1 Introduction
- 2 Two-electron anisotropic quantum dot model 3D \rightarrow quasi 1D
- 3 Resonances

Outline

- 1 Introduction
- 2 Two-electron anisotropic quantum dot model 3D \rightarrow quasi 1D
- 3 Resonances
- 4 Results for quasi-1D Gaussian QDs
 - Resonance energies and widths
 - Entanglement entropies

Outline

- 1 Introduction
- 2 Two-electron anisotropic quantum dot model 3D \rightarrow quasi 1D
- 3 Resonances
- 4 Results for quasi-1D Gaussian QDs
 - Resonance energies and widths
 - Entanglement entropies
- 5 Comparison with the solvable 2-particle model

Outline

- 1 Introduction
- 2 Two-electron anisotropic quantum dot model 3D \rightarrow quasi 1D
- 3 Resonances
- 4 Results for quasi-1D Gaussian QDs
 - Resonance energies and widths
 - Entanglement entropies
- 5 Comparison with the solvable 2-particle model
- 6 Summary

Introduction

Natural and artificial N particle quantum systems

- **Natural**

few-electron atoms and ions
few-electron molecules
few-nucleon nuclei

} parameters fixed by God

- **Artificial**

few ions in traps
ultracold few-atom systems
few-electron quantum dots (QDs)
...

} parameters fixed by experimentalists

The systems are modelled by the Schrödinger N -body equation

$$\hat{H} = \sum_{i=1}^N \left[-\frac{\hbar^2}{2m} \nabla_i^2 + V(\mathbf{r}_i) \right] + \frac{1}{2} \sum_{i=1, i \neq j}^N U(|\mathbf{r}_i - \mathbf{r}_j|)$$

Two-electron anisotropic quantum dot model

3D \rightarrow quasi 1D

Model Hamiltonian

$$\hat{H} = \sum_{i=1}^2 \left[-\frac{\hbar^2 \nabla_i^2}{2m^*} + U(x_i, y_i, z_i) \right] + \frac{\kappa}{|\mathbf{r}_1 - \mathbf{r}_2|},$$

m^* - the effective electron mass

$\kappa = \frac{e^2}{\epsilon^*}$, where ϵ^* - the effective dielectric constant

e.g. for GaAs QD: $m^* = 0.067m_e$, $\epsilon^* = 11$

3D two-electron QD

Model Hamiltonian

$$\hat{H} = \sum_{i=1}^2 \left[-\frac{\hbar^2 \nabla_i^2}{2m^*} + U(x_i, y_i, z_i) \right] + \frac{\kappa}{|\mathbf{r}_1 - \mathbf{r}_2|},$$

m^* - the effective electron mass

$\kappa = \frac{e^2}{\epsilon^*}$, where ϵ^* - the effective dielectric constant

e.g. for GaAs QD: $m^* = 0.067m_e$, $\epsilon^* = 11$

Anisotropic QD

$$\hat{H} = \sum_{i=1}^2 \left[-\frac{\hbar^2 \nabla_i^2}{2m^*} + U_{\perp}(x_i, y_i) + U_{\parallel}(z_i) \right] + \frac{\kappa}{|\mathbf{r}_1 - \mathbf{r}_2|},$$

Lateral confinement: $U_{\perp}(x, y) = \frac{m^* \omega^2}{2}(x^2 + y^2)$

Longitudinal potential: $U_{\parallel}(z_i)$

Quasi-1D QD

Strongly anisotropic QD

Lateral confinement much stronger than the longitudinal one.

Single mode approximation: $\Psi(\mathbf{r}_1, \mathbf{r}_2) \cong \psi(z_1, z_2)\phi(x_1)\phi(y_1)\phi(x_2)\phi(y_2)$, where

$$\phi(x) = \left(\frac{m^* \omega}{\hbar \pi}\right)^{\frac{1}{4}} e^{-\frac{m^* \omega x^2}{2\hbar}}$$

Longitudinal motion

$$H_{\parallel} = \sum_{i=1}^2 \left[-\frac{\hbar^2}{2m^*} \frac{\partial^2}{\partial z_i^2} + U_{\parallel}(z_i) \right] + V_{\text{eff}}(z) + 2\hbar\omega$$

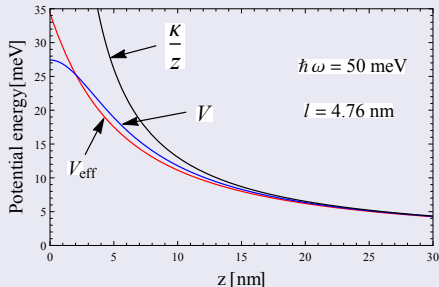
Effective electron-electron interaction

$$V_{\text{eff}}(z) = \kappa \int d^2x d^2y \frac{|\phi(x_1)\phi(x_2)\phi(y_1)\phi(y_2)|^2}{\sqrt{(x_1-x_2)^2 + (y_1-y_2)^2 + z^2}}$$

approximated by truncated Coulomb potential

$$V(z) = \frac{\kappa}{\sqrt{z^2 + l^2}}$$

l - the lateral radius



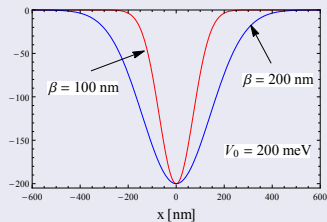
Attractive Gaussian potential

Longitudinal confinement

$$U_{\parallel}(x) = -V_0 e^{-\frac{x^2}{\beta^2}}$$

β - the range of the longitudinal confinement

V_0 - the depth of the potential well



Quasi-1D QD

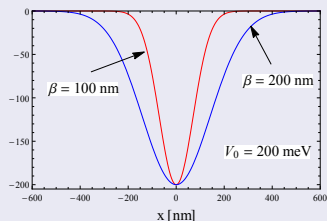
Attractive Gaussian potential

Longitudinal confinement

$$U_{\parallel}(x) = -V_0 e^{-\frac{x^2}{\beta^2}}$$

β - the range of the longitudinal confinement

V_0 - the depth of the potential well



Dimensionless Hamiltonian

After rescaling $x \rightarrow \beta x$, $V_0 \rightarrow \frac{\hbar^2}{m\beta^2} V_0$, $E \rightarrow \frac{\hbar^2}{m\beta^2} E$

$$\hat{H} = \sum_{i=1}^2 \left[-\frac{1}{2} \frac{\partial^2}{\partial x_i^2} - V_0 e^{-x_i^2} \right] + \frac{g}{\sqrt{(x_1 - x_2)^2 + \delta}}$$

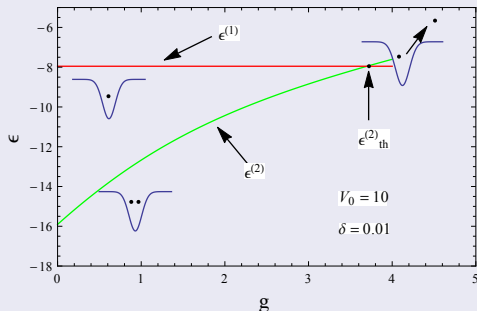
g - ratio of the interaction to the confinement strength

$\sqrt{\delta} \approx$ lateral radius

Autoionisation

Two-particle spectrum

The spectrum is continuous above the threshold energy $\epsilon_{th}^{(2)} = \epsilon^{(1)}$ where $\epsilon^{(1)}$ is the lowest one-particle energy.



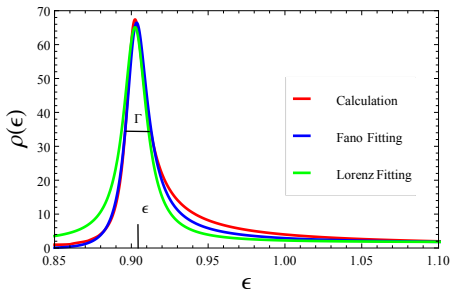
autoionizing resonances

Resonances

Mathematical description of resonances

Resonances are localized metastable states with finite lifetime.

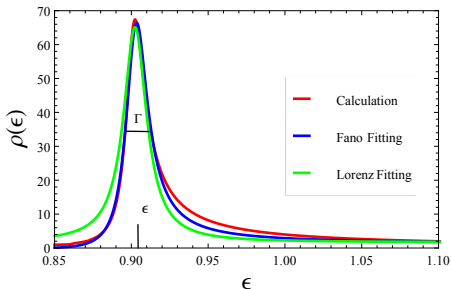
Experimental manifestation of resonance phenomena: peaks in the collision cross sections well described by two-parameter formulas (Breit-Wigner, Fano,...).



Mathematical description of resonances

Resonances are localized metastable states with finite lifetime.

Experimental manifestation of resonance phenomena: peaks in the collision cross sections well described by two-parameter formulas (Breit-Wigner, Fano,...).



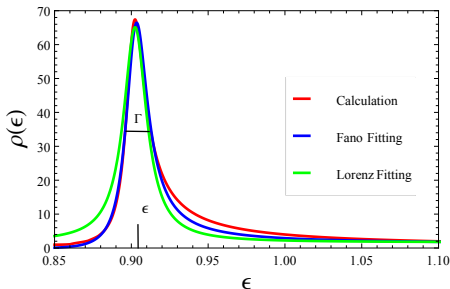
G.Gamow (1928): The peak position ϵ and the width Γ may be related to the complex eigenvalues $E = \epsilon - i\Gamma/2$ of the Schrödinger equation

$$\hat{H}\psi = E\psi$$

Mathematical description of resonances

Resonances are localized metastable states with finite lifetime.

Experimental manifestation of resonance phenomena:
peaks in the collision cross sections well described by two-parameter formulas (Breit-Wigner, Fano,...).



G.Gamow (1928): The peak position ϵ and the width Γ may be related to the complex eigenvalues $E = \epsilon - i\Gamma/2$ of the Schrödinger equation

$$\hat{H}\psi = E\psi$$

Probability density: $|\psi(x, t)|^2 = e^{-\frac{\Gamma}{\hbar}t} |\psi(x)|^2$,

thus $\Gamma = \frac{\hbar}{\tau}$, where τ is the resonance lifetime.

Determination of of resonant states

Asymptotics of resonance wave functions

$\lim_{x \rightarrow \infty} \psi_{res}(x) \propto e^{ik_{res}x}$, where $k_{res} = |k_{res}|e^{-i\alpha_{res}}$ with $0 < \alpha_{res} < \frac{\pi}{4}$

$$\psi_{res}(x \rightarrow \infty) \propto e^{i|k_{res}| \cos \alpha_{res} x} e^{|k_{res}| \sin \alpha_{res} x} \rightarrow \infty$$

Resonant wave function $\psi_{rez}(x)$ diverges exponentially, so doesn't belong to the Hilbert space. The Hamiltonian is thus not hermitian.

Determination of of resonant states

Asymptotics of resonance wave functions

$\lim_{x \rightarrow \infty} \psi_{res}(x) \propto e^{ik_{res}x}$, where $k_{res} = |k_{res}|e^{-i\alpha_{res}}$ with $0 < \alpha_{res} < \frac{\pi}{4}$

$$\psi_{res}(x \rightarrow \infty) \propto e^{i|k_{res}| \cos \alpha_{res} x} e^{|k_{res}| \sin \alpha_{res} x} \rightarrow \infty$$

Resonant wave function $\psi_{rez}(x)$ diverges exponentially, so doesn't belong to the Hilbert space. The Hamiltonian is thus not hermitian.

Methods:

Hermitian QM

- Wavepacket propagation with outgoing boundary conditions
- Complex poles of the scattering matrix
- Real stabilization method
- Rigged Hilbert space (Berggren representation)
- ...

Non-Hermitian QM

- Complex scaling
- Complex absorbing potential
- ...

Complex scaling

Complex rotation: $\hat{U} = e^{-\theta \hat{x} \hat{p} / \hbar}$, $\hat{x} \rightarrow U \hat{x} U^{-1} = e^{i\theta} \hat{x}$

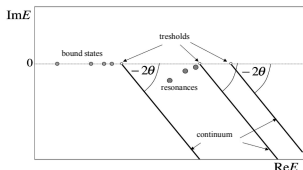
$$\hat{H} \rightarrow \hat{U} \hat{H} \hat{U}^{-1} = \hat{H}_\theta = -\frac{\hbar^2}{2m} e^{-2i\theta} \nabla^2 + V(e^{i\theta} x)$$

Asymptotics of rescaled wave function

$$\psi_{res}^\theta(x \rightarrow \infty) \rightarrow e^{i|k_{res}| \cos(\theta - \alpha_{res})x} e^{-|k_{res}| \sin(\theta - \alpha_{res})x} \rightarrow 0, \text{ if } 0 < \theta - \alpha_{res} < \pi/2.$$

Theorem E. Balslev, J.M. Combes, Commun. Math. Phys. 22 (1971) 280

The spectrum of the complex-rotated non-hermitian Hamiltonian $\hat{H}_\theta \psi^\theta = E \psi^\theta$



- Bound-state eigenvalues, the complex resonance eigenvalues and the thresholds are the same as those of the original Hamiltonian
- The continuous spectra are rotated about the thresholds by an angle 2θ into the lower energy half-plane

Advantage: resonances can be determined as the eigenstates of \hat{H}_θ with complex energy $E = ReE - i ImE = \epsilon - i \frac{\Gamma}{2}$ by using bound-state-like strategies.

Probability density $|\psi(\mathbf{r}, t)|^2 = e^{-\frac{\Gamma}{\hbar} t} |\psi(\mathbf{r})|^2$ decays with a lifetime τ , where $\Gamma = \frac{\hbar}{\tau}$.

CI method for bound states

To determine the spectrum of our system, we apply the configuration interaction (CI) expansion

$$\Psi(x_1, x_2) = \sum_{i,j} a_{ij} \psi_{ij}(x_1, x_2)$$

where the basis functions are given by

$$\psi_{ij}(x_1, x_2) = c_{ij} (\phi_i(x_1)\phi_j(x_2) \pm \phi_j(x_1)\phi_i(x_2)), \text{ where } c_{ij} = \begin{cases} \frac{1}{\sqrt{2}} & i \neq j \\ \frac{1}{2} & i = j \end{cases},$$

which ensures the proper symmetry under permutations of the particles, so that (+) and (-) correspond to the singlet and triplet states, respectively.

The single particle basis is taken as composed of harmonic oscillator eigenfunctions

$$\phi_i^\Omega(x) = \left(\frac{\sqrt{\Omega}}{\sqrt{\pi} 2^{i/2} i!} \right)^{1/2} H_i(\sqrt{\Omega}x) e^{-\frac{\Omega x^2}{2}}$$

with an arbitrary frequency Ω . We determine the eigenstates of the system through diagonalization of the truncated Hamiltonian matrix $[H^\Omega]_{M \times M}$, the elements of which are given by

$$H_{nmij}^\Omega = \int_{-\infty}^{\infty} \psi_{nm}^\Omega(x_1, x_2) \hat{H} \psi_{ij}^\Omega(x_1, x_2) dx_1 dx_2.$$

In determining bound-states, the nonlinear parameter Ω is considered as a real and positive number. Its value is fixed so as to minimize the considered energy eigenvalue:

$$\frac{dE_k}{d\Omega} = 0.$$

CI method for resonant states

The CI method can be generalised to the case of resonant states, by allowing the nonlinear parameter to be a complex number $\Omega = \alpha e^{-2i\theta}$.

CI method for resonant states

The CI method can be generalised to the case of resonant states, by allowing the nonlinear parameter to be a complex number $\Omega = \alpha e^{-2i\theta}$.

Justification by the complex basis approach

N. Moiseyev, Mol. Phys., 47, (1982) 585

The nonlinear parameter Ω in HO eigenfunctions is the scale parameter:

$$\phi_j^\Omega(x) = \frac{1}{\sqrt{\Omega}} \phi_j\left(\frac{x}{\Omega}\right), \text{ where } \phi_i(x) = \left(\frac{1}{\sqrt{\pi 2^i i!}}\right)^{1/2} H_i(x) e^{-\frac{x^2}{2}}.$$

The matrix elements of the complex scaled ($x \mapsto \eta e^{i\theta} x$) Hamiltonian

$$H_{ij}^\theta = \langle \phi_i | \hat{H}^\theta | \phi_j \rangle = \int \phi_i(x) \left[-\frac{\hbar^2}{2m} \frac{e^{-2i\theta}}{\eta^2} \frac{\partial^2}{\partial x^2} + V(\eta e^{i\theta} x) \right] \phi_j(x) dx,$$

can be equivalently obtained in the complex basis approach

$$H_{ij}^\Omega = \langle \phi_i^\Omega | \hat{H} | \phi_j^\Omega \rangle = \int \phi_i^\Omega(x) \left[-\frac{\hbar^2}{2m} \frac{\partial^2}{\partial x^2} + V(x) \right] \phi_j^\Omega(x) dx = \int \phi_i(x) \left[-\frac{\hbar^2}{2m} \Omega \frac{\partial^2}{\partial x^2} + V\left(\frac{x}{\sqrt{\Omega}}\right) \right] \phi_j(x) dx$$

\uparrow
 $x \mapsto \sqrt{\Omega} x$

$$\Omega = \frac{e^{-2i\theta}}{\eta^2} = \alpha e^{-2i\theta}$$

We will study

Hamiltonian

$$\hat{H} = \sum_{i=1}^2 \left[-\frac{1}{2} \frac{\partial^2}{\partial x_i^2} - V_0 e^{-x_i^2} \right] + \frac{g}{\sqrt{(x_1 - x_2)^2 + \delta}}$$

lowest singlet (spatially symmetric) and triplet (spatially antisymmetric) states

We will study

Hamiltonian

$$\hat{H} = \sum_{i=1}^2 \left[-\frac{1}{2} \frac{\partial^2}{\partial x_i^2} - V_0 e^{-x_i^2} \right] + \frac{g}{\sqrt{(x_1 - x_2)^2 + \delta}}$$

lowest singlet (spatially symmetric) and triplet (spatially antisymmetric) states

CI method

The eigenstates of the system determined through diagonalization of the truncated Hamiltonian matrix $[H^\Omega]_{M \times M}$, the elements of which are given by

$$H_{nmij}^\Omega = \int_{-\infty}^{\infty} \psi_{nm}^\Omega(x_1, x_2) \hat{H} \psi_{ij}^\Omega(x_1, x_2) dx_1 dx_2.$$

Both bound and resonant states obtained with the value of the nonlinear parameter set to Ω_{opt} that fulfils the stationarity equation

$$\left. \frac{dE_k^\Omega}{d\Omega} \right|_{\Omega=\Omega_{opt}} = 0.$$

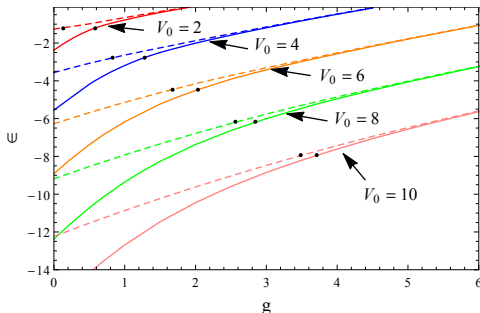
For bound-states the nonlinear parameter Ω_{opt} is a real and positive number. For resonances it turns out to be a complex number $\Omega_{opt} = \alpha_{opt} e^{-2i\theta_{opt}}$, which results in complex energy eigenvalues. The convergent results obtained with the Hamiltonian matrix $[H^{\Omega_{opt}}]_{M \times M}$ of dimension $M = 324$ for the triplet state and $M = 342$ for singlet state.

Results for quasi-1D Gaussian QDs

Resonance energies and widths

The effect of V_0 on energies

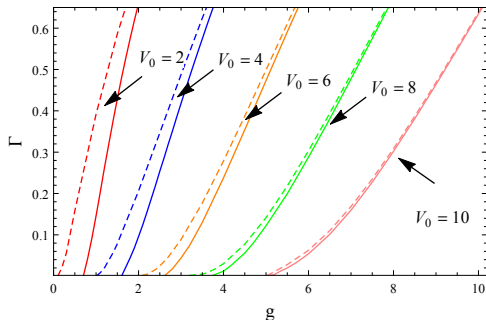
The analysis of the effect of the depth of the longitudinal trapping potential on the spectrum performed at fixed confinement anisotropy $\delta = 0.01$. The black points represent the thresholds g_{th} which separate bound states from resonances.



- The triplet thresholds are lower than the singlet ones and the differences between them decrease for increasing V_0 .
- The energies of singlet states lie below the corresponding triplet ones and the singlet-triplet degeneracy is achieved in the limit of $g \rightarrow \infty$.

The effect of V_0 on resonance width

Above the autoionisation thresholds, the energy eigenvalues acquire an imaginary part which determines the width Γ of the corresponding resonance state.

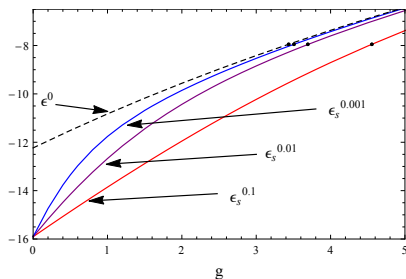


- The lifetime of resonant states increases with increasing V_0 and decreasing g .
- The singlets decay faster than the corresponding triplets, but the differences diminish with increasing depth of the trap.

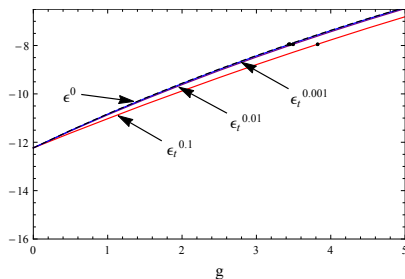
The effect of the lateral radius δ on the energy

The influence of confinement anisotropy studied for a trap of fixed depth $V_0 = 10$.

singlet energies ϵ_s^δ



triplet energies ϵ_t^δ



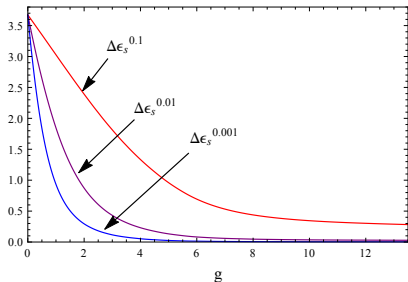
- Both the singlet and triplet energies monotonically increase when δ decreases.
- The threshold values of the interaction strength g_{th}^δ , which separate bound states from resonances, get smaller with decreasing δ .

For the pure Coulomb interaction $\delta = 0$, the singlet and triplet energies are degenerate ($\epsilon_s^0 = \epsilon_t^0$), except at the point $g = 0$ where the dependence of the singlet energy on δ is discontinuous.

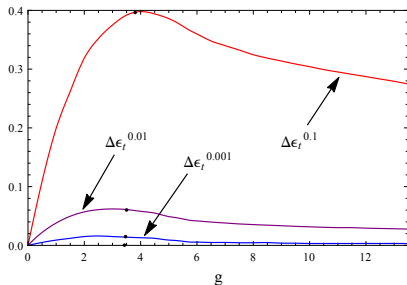
Energy differences $\Delta\epsilon_{s,t}^\delta = \epsilon^0 - \epsilon_{s,t}^\delta$

The influence of confinement anisotropy studied for a trap of fixed depth $V_0 = 10$.

singlet energy differences $\Delta\epsilon_s^\delta$



triplet energy differences $\Delta\epsilon_t^\delta$



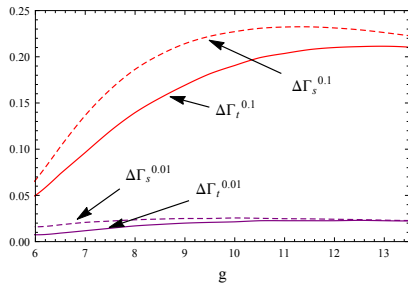
In the triplet case, the energy differences are maximal in the vicinity of autoionization thresholds.

The differences of the resonance widths

The influence of confinement anisotropy studied for a trap of fixed depth $V_0 = 10$.

The differences of the resonance widths

$$\Delta\Gamma_{s,t}^\delta = \Gamma^0 - \Gamma_{s,t}^\delta,$$



where Γ^0 is for pure Coulomb interaction.

- After initially increasing, the differences $\Delta\Gamma_{s,t}^\delta$ go through the maxima and then slowly decrease with increasing g .
- For smaller values of the cut-off parameter δ the differences are smaller.

Results for quasi-1D Gaussian QDs

Entanglement entropies

One-particle entanglement

One-particle reduced density matrix **1-RDM**

$$\rho(\mathbf{r}_1, \mathbf{r}'_1) = \int \Psi(\mathbf{r}_1, \mathbf{r}_2, \dots, \mathbf{r}_N) \Psi(\mathbf{r}'_1, \mathbf{r}_2, \dots, \mathbf{r}_N) d^3 r_2 \dots d^3 r_N$$

One-particle entanglement

One-particle reduced density matrix **1-RDM**

$$\rho(\mathbf{r}_1, \mathbf{r}'_1) = \int \Psi(\mathbf{r}_1, \mathbf{r}_2, \dots, \mathbf{r}_N) \Psi(\mathbf{r}'_1, \mathbf{r}_2, \dots, \mathbf{r}_N) d^3 r_2 \dots d^3 r_N$$

admits a Schmidt decomposition:

$$\rho(\mathbf{r}, \mathbf{r}') = \sum \lambda_k u_k(\mathbf{r}) u_k(\mathbf{r}'), \quad \sum \lambda_k = 1.$$

Entanglement spectrum: the occupancies $\{\lambda_k\}$ of natural orbitals $\{u_k(\mathbf{r})\}$ characterise entanglement between **one of the particles** and **the rest of the system**.

One-particle entanglement

One-particle reduced density matrix 1-RDM

$$\rho(\mathbf{r}_1, \mathbf{r}'_1) = \int \Psi(\mathbf{r}_1, \mathbf{r}_2, \dots, \mathbf{r}_N) \Psi(\mathbf{r}'_1, \mathbf{r}_2, \dots, \mathbf{r}_N) d^3 r_2 \dots d^3 r_N$$

admits a Schmidt decomposition:

$$\rho(\mathbf{r}, \mathbf{r}') = \sum \lambda_k u_k(\mathbf{r}) u_k(\mathbf{r}'), \quad \sum \lambda_k = 1.$$

Entanglement spectrum: the occupancies $\{\lambda_k\}$ of natural orbitals $\{u_k(\mathbf{r})\}$ characterise entanglement between **one of the particles** and **the rest of the system**.

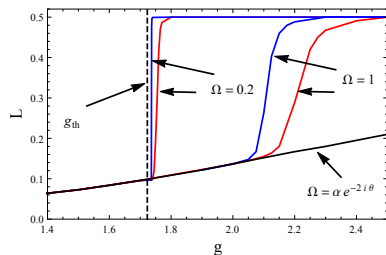
Measures based on 1-RDM:

- von Neumann entropy: $\mathbf{S} = -\text{Tr}[\rho \ln \rho] = -\sum \lambda_k \ln \lambda_k$
- linear entropy: $\mathbf{L} = 1 - \text{Tr} \rho^2 = 1 - \sum \lambda_k^2$
- Rényi entropies: $\lim_{n \rightarrow 1} \mathbf{S}_n = \mathbf{S}$
 $\mathbf{S}_2 = -\ln(1 - \mathbf{L})$
 $\mathbf{S}_3 \dots$
- ... $\mathbf{S}_q = \frac{1}{1-q} \ln \text{Tr}(\rho^q) = \frac{1}{1-q} \ln \sum \lambda_k^q$

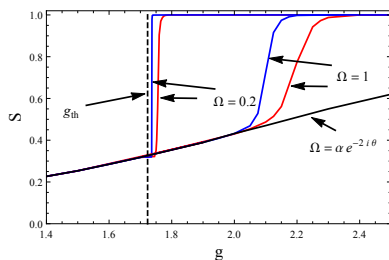
Entanglement entropies calculated by real stabilization method

$$V_0 = 4 \text{ and } \delta = 0.1$$

real linear entropy



real von Neumann entropy

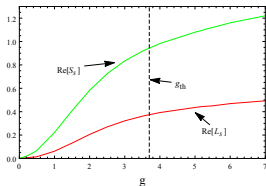


Entropies calculated by real stabilization method provide information on critical behavior of the two-particle QD.

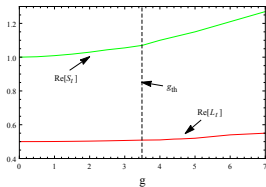
Entanglement entropies calculated by complex scaling

$$V_0 = 10 \quad \delta = 0.01$$

Real part of linear and von Neumann entropies of the singlet state



Real part of linear and von Neumann entropies of the triplet state



Real parts of entropies calculated by complex scaling are smooth functions of the interaction strength g . The entropies acquire imaginary parts at autoionization thresholds.

Entanglement entropies in the Moshinsky model

Moshinsky model

N-particle Moshinsky Hamiltonian

Heisenberg 1926, Moshinsky 1968

Confined by $V(x) = \frac{m\Omega^2 x^2}{2}$, interacting via $U(x_i, x_j) = \lambda(x_i - x_j)^2$

Rescaled Hamiltonian ($x \mapsto \sqrt{\frac{\hbar}{m\Omega}} x$, $E \mapsto \hbar\Omega E$)

$$H = \sum_{i=1}^N \left[-\frac{\nabla_i^2}{2} + \frac{1}{2} x_i^2 \right] + g \sum_{i < j} (x_i - x_j)^2,$$

where $g = \frac{\lambda}{m\Omega^2}$ - interaction / trapping strength; $g < 0$ - repulsive interaction

Analytic solution: ground state

$$\omega = \sqrt{1 + 2Ng} \quad g_{\text{critical}} = -\frac{1}{2N}$$

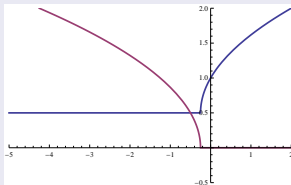
exact wave function: $\psi(Y, r) = \left(\frac{\omega}{\pi}\right)^{\frac{N-1}{4}} e^{-\frac{\omega r^2}{2}} \left(\frac{1}{\pi}\right)^{\frac{1}{4}} e^{-\frac{Y^2}{2}}$, where $r^2 = \sum_{i=2}^N y_i^2$

exact energy: $E = \frac{1}{2}(N-1)\omega + \frac{1}{2}$.

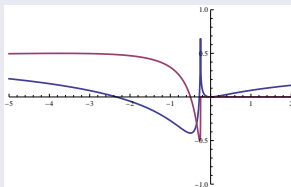
exact linear entropy: $L = 1 - N \sqrt{\frac{\omega}{\omega(N^2 - 2N + 2) + 2(gN + 1)(N - 1)}}$

Moshinsky model $N = 2$: $g_{critical} = -\frac{1}{4}$

exact energy: $E = \frac{1}{2}\sqrt{4g+1} + \frac{1}{2}$.

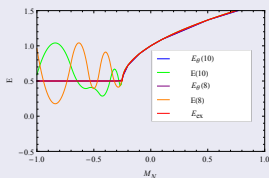


exact linear entropy: $L = \frac{\sqrt{2g+\sqrt{4g+1}+1}-\sqrt{2}^4\sqrt{4g+1}}{\sqrt{2g+\sqrt{4g+1}+1}}$

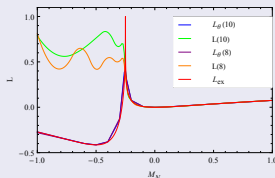


CI results for the Moshinsky model $N = 2$

Real part of the lowest energy: $E = \frac{1}{2}\sqrt{4g+1} + \frac{1}{2}$.



Real part of the linear entropy: $L = \frac{\sqrt{2g+\sqrt{4g+1}+1}-\sqrt{2}\sqrt[4]{4g+1}}{\sqrt{2g+\sqrt{4g+1}+1}}$



quasi-1D Gaussian QD

- The depth of the longitudinal trapping potential has an important effect on the critical value of the interaction strength g_{th} at which the bound state is transformed into a resonance, namely the larger is the value of V_0 , the larger is g_{th} .
- The impact of the lateral radius of the quasi-1D QD is the most visible near the ionization thresholds for triplet states.
- Entanglement entropies calculated by real stabilization method show a critical behavior at the autoionization threshold.
- Entanglement entropies calculated by complex scaling acquire the imaginary part at the autoionization threshold, but their real parts don't show a critical behavior there.

Summary

quasi-1D Gaussian QD

- The depth of the longitudinal trapping potential has an important effect on the critical value of the interaction strength g_{th} at which the bound state is transformed into a resonance, namely the larger is the value of V_0 , the larger is g_{th} .
- The impact of the lateral radius of the quasi-1D QD is the most visible near the ionization thresholds for triplet states.
- Entanglement entropies calculated by real stabilization method show a critical behavior at the autoionization threshold.
- Entanglement entropies calculated by complex scaling acquire the imaginary part at the autoionization threshold, but their real parts don't show a critical behavior there.

Moshinsky model

- Entanglement entropies calculated by real stabilization method show a critical behavior at $g_{critical}$.
- Entanglement entropies calculated by complex scaling tend to the exact results. Entropies acquire the imaginary part at $g_{critical}$, and their real parts show a critical behavior there.